

Galaxy Cluster Cosmic-rays, Hot Gas, X-rays and Collisions

T.J. Sumner, J.J. Quenby, R. Bossart, D. Farrah, and M. Hernandez

Physics Department, Imperial College, Prince Consort Rd., London, SW7 2BZ, UK

E-mail: t.sumner@ic.ac.uk

Abstract

Excess EUV radiation from some clusters of galaxies accessible to ROSAT measurements in the 100-1000 eV energy range is reanalysed employing multi-temperature, thin plasma code emission fits. For both clusters, A1795 and Virgo, two hot components, with $\log T \sim 7.8$ and 6.6, and a warm component, with $\log T \sim 5.7$, are found. The two hot components are discussed in terms of a cluster-cluster collision model. The warm component for A1795 is reanalysed in terms of a broken power law, which could be ascribed to inverse Compton radiation arising from CMB interaction with a relativistic intergalactic cosmic-ray gas. It is suggested that the warm component from the Virgo central region is due to cosmic-rays escaping from M87. This lessens the argument requiring baryonic matter as the dominant mass component of A1795 or Virgo.

1 Introduction:

Soft x-ray emission from the intergalactic gas of clusters apparently provides a measure of the dominant baryonic component in the universe. Typically, the ratio of hot gas to stellar mass is 2–10, while the gas to virial mass ratio is 0.1–0.2. There is a discrepancy (Krauss, 1997), however, between the limiting primordial nucleosynthesis value of $\Omega_B \leq 0.026h^{-2}$ and the x-ray cluster value $\Omega_B \leq 0.05h^{-1.5}$. A possibly even more difficult problem arises from the work of Lieu et al (1996) who found, using data from the EUVE satellite, soft, extreme ultraviolet radiation which implied cooling flows well in excess of those derived from x-ray observations at higher energies. In some cases the cooling flow appeared sufficient to provide the whole cluster virial mass during its lifetime. The usual model for the hot cluster gas is a hydrostatic equilibrium between the underlying gravitational field and the gas pressure gradient with the x-ray emission being given by thin plasma thermal bremsstrahlung plus line emission appropriate to the expected gas ionisation states. Early work on clusters considered an alternative, Inverse Compton model (Harris & Romanishin, 1974, Carpenter et al, 1976) which we will return to in attempting to remove the problem of over-abundant baryons.

2 Analysis of Abell 1795 and Virgo Cluster Emission:

Corrected ROSAT PSPC spectral data were extracted for various cluster regions. Background due to emissions other than from the cluster were established by modelling the soft x-ray flux with a series of slabs (Sidher et al 1996, 1999). The furthest slab defines the soft x-ray extragalactic background, taken to be the power law, $0.01E^{-1.4} \text{ ph cm}^{-2} \text{ s}^{-1} \text{ keV}^{-1} \text{ sr}^{-1}$. Next come two slabs representing a hot Galactic halo and the absorption of the galactic disk and finally the closest slab represents the hot gas of the local bubble with a small amount of intermixed absorbing material. The radiation transfer through each slab is given by

$$I_f(E) = I_i(E)e^{-n_H\sigma(E)l} + \frac{n_e^2 P(E, T)}{n_H \sigma(E)} (1 - e^{-n_H\sigma(E)l}) \quad (1)$$

The Landini-Fossi (L-F) plasma code is used to model the hot gas emission components while the HI absorption column in the disk is derived from the Stark and Dwingeloo catalogues. The local bubble temperature is well determined at $\log T = 5.9$ and the column density is taken as 6.6×10^{18} , (Juda et al 1991, Lieu et al 1992). All other parameters, that is the emission measures for the local bubble and halo and the

halo temperature, are allowed to vary and a fitting scheme is implemented to obtain values suitable for directions close to the immediate surroundings of the cluster.

Excess cluster emission over the nearby background is modelled by extra slabs, which are added as required at different positions in the cluster. Previous work (Lieu et al 1996) has demonstrated the need for a warm, EUV component as well as the x-ray hot component of the cluster gas usually assumed in isothermal, hydrostatic equilibrium models. Our analysis confirms the need for an EUV component and requires a multi-temperature hot component. We consider an inverse Compton interpretation of the EUV part of the excess, and allow this component to be represented as a broken power law, in which the break corresponds to a possible cut-off in the spectrum at high electron energy. In the following, three extra x-ray emitting slabs are employed, two assuming L-F type thin-plasma emission while the third is either a representation based also on L-F emission or a broken power law. Table 1 lists the fits obtained, all with reduced χ^2 values ≤ 2 , from 11 positions along a line scan across A1795 with a field of view 0.1° diameter. The central position coincides with the cluster centre and the whole scan covers 1° of arc. Temperatures are given as $\log T$ in K and the emission measures, EM, are in units of $10^{-2} \text{ cm}^{-6} \text{ pc}$.

We note, first there is a small drop in the temperature of the hot component around the centre of the cluster where the emission is highest, $\log T$ going down from 7.9 to 7.7. Second, another hot component with $\log T \approx 6.6$ is required in the central region, but with an emission measure about $1/20^{\text{th}}$ of the dominating component. Third, the EUV emission with $\log T \approx 5.7$ is found at all positions, but with a relatively greater importance at the extremities of the cluster. Figure 1 shows the variation in emission measure of the two hot components as a function of region in the scan in galactic longitude across A1795, according to Table 1.

Table 1: 3-Slab L-F Model for A1795.

| Region | T_1 | EM_1 | T_2 | EM_2 | T_3 | EM_3 |
|--------|-------|--------|-------|--------|-------|--------|
| 1 | 7.9 | 8 | 5.9 | 6 | | |
| 2 | 7.9 | 18 | 5.9 | 8 | | |
| 3 | 7.9 | 35 | 5.8 | 15 | | |
| 4 | 7.9 | 92 | 5.7 | 43 | | |
| 5 | 7.8 | 515 | 6.5 | 18 | 5.7 | 205 |
| 6 | 7.7 | 1790 | 6.6 | 80 | 5.7 | 690 |
| 7 | 7.7 | 1275 | 6.7 | 70 | 5.7 | 520 |
| 8 | 7.7 | 132 | 5.7 | 60 | | |
| 9 | 7.9 | 44 | 5.7 | 28 | | |
| 10 | 7.9 | 18 | 5.7 | 23 | | |
| 11 | 7.9 | 8 | 5.7 | 14 | | |

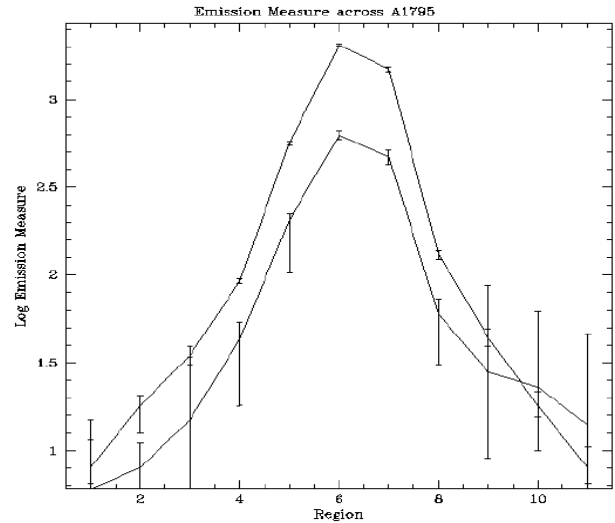


Figure 1: Emission measure variation across A1795

A good alternative fit to the A1795 data in the central region 6 is found if we simply replace the third L-F slab at $\log T = 5.7$ with a broken power law defined by $1.1 \times 10^{-4} E^{-7.7} \text{ ph cm}^{-2} \text{ s}^{-1} \text{ keV}^{-1} \text{ sr}^{-1}$ for $E \leq 1 \text{ keV}$ and with the slope decreasing to an exponent of $-10 > 1 \text{ keV}$. The two fits are shown in Figure 2 where the data points are seen with error bars. The two solid curves correspond to the sum of all three slabs fitting the central cluster region and the dashed curve and the dot-dash curves respectively illustrate the third L-F slab and the broken power law slab fits employed. All points are folded through the PSPC response.

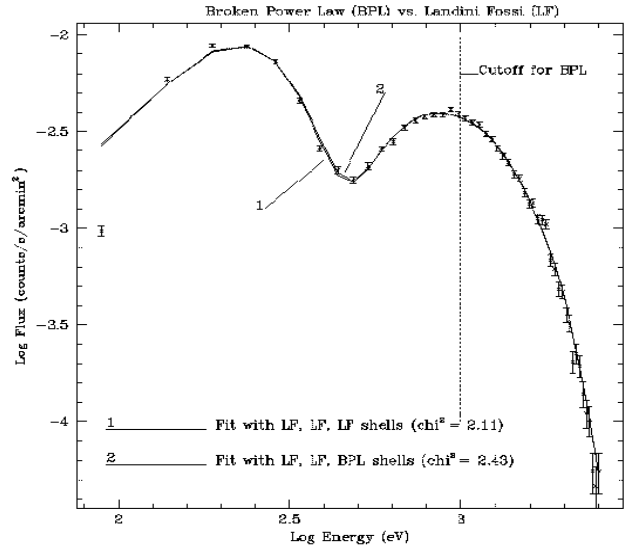
Table 2 lists L-F 3-slab fits to some Virgo cluster data. They are for two outer regions, 0.2° radius, $\sim 40'$ from the centre, two inner regions, 0.1° radius $\sim 10'$ from the centre and the region centred on M87, of 0.075° radius. Units are $\log T$ in K and emission measure, EM, in 10^{16} cm^{-5} .

In contrast to the A1795 results, Virgo shows no central temperature drop of the hottest component ($\log T \approx 7.4$), but in other respects, the emission is qualitatively similar, there being both a second hot component near the centre at $\log T \approx 6.8$ and an EUV component with $\log T \approx 5.7$, the latter however not obviously reaching the outermost regions.

Table 2: 3-Slab L-F Model for Virgo.

| Region | T ₁ | EM ₁ | T ₂ | EM ₂ | T ₃ | EM ₃ |
|------------------|----------------|-----------------|----------------|-----------------|----------------|-----------------|
| Outer | 7.4 | 16.1 | | | | |
| | 7.4 | 13.6 | | | | |
| Inner | 7.5 | 389 | 6.5 | 16 | 5.7 | 95 |
| | 7.5 | 351 | 6.7 | 15 | 5.8 | 75 |
| Central (M87) | 7.4 | 1996 | 6.9 | 646 | 5.7 | 490 |

Figure 2: Broken power-law fits compared to L-F fits



3 Non-Equilibrium and Cosmic Ray Effects:

3.1 Cluster-Cluster Collisions: The hottest x-ray component and warm EUV component results are similar to those previously summarised by Sarazin & Lieu (1998). They note for A1795 that the implied cooling flow of the warm component if taken over the age of the Universe requires a total flow mass equivalent to the Virial mass of the cluster. However, the presence of a multi-temperature hot component, together with a warm component, casts doubt on the equilibrium model. Cosmic evolution allows for cluster collisions or mergers and numerical simulations illustrate the effects (Schindler & Muller 1993). These predictions for the collision of two sub clusters reveal extra heating at the centre, asymmetry in the temperature and density distribution and the development of rather cool areas post shock. Many lines of sight viewing the x-ray emission from central regions would see a factor 10 in temperature range while the total x-ray emission varies by nearly a factor two over 10^9 years.

The results of Tables 1 and 2 indeed show two temperatures in the central regions, differing by a factor 10. Figure 1 shows evidence of asymmetry in the emission measures of the hot components. We conclude that there is sufficient qualitative similarity between the observations of A1795 and Virgo and the cluster-cluster collision model to claim both clusters have suffered major dynamical processes over the last 10^9 years. Such processes will invalidate total baryonic mass and cooling estimates based upon equilibrium models.

3.2 Inverse Compton Contribution: It has been pointed out (Sarazin & Lieu 1998) that cosmic ray electrons of Lorentz factor γ interact with the cosmic microwave background to produce EUV photons of energy $h\nu_{EUV}$ by inverse Compton (IC) according to

$$\gamma = 300 \left(\frac{h\nu_{EUV}}{75\text{eV}} \right)^{0.5} \quad (2)$$

The lifetime against the IC effect is currently $2 \times 10^{12} \gamma^{-1}$ yr, but since this is inversely proportional to the CMB density which is, in turn, proportional to $(1+z)^4$, only electrons from $z < 2$ can contribute to the EUV flux. The intra-cluster cosmic-ray electron energy in A1795 needs to be $1/10^{\text{th}}$ that of the thermal gas energy in order to explain the EUV flux. By comparison, the cosmic-ray electron energy density in our

galaxy is about $1/10^{\text{th}}$ of the cosmic-ray proton energy density, which is in turn about equal to the galactic gas thermal energy density. Thus there may be little room to reduce the total baryonic content of the cluster since we seem to need to keep the gas content high if the precedence set by our galaxy is followed.

Further constraints for the IC model arise from the power law EUV emission fit found for A1795. The photon spectral energy index corresponds to an electron spectral index which is rather steeper compared to the non-relativistic, test-particle value for the diffusive shock model of particle acceleration in the strong shock limit of -2. The break at 1 keV corresponds to $\gamma = 10^3$. This value can be related to the lifetime against Coulomb collision loss in the intra-cluster medium,

$$t_c \approx 7 \times 10^9 \frac{\gamma}{300} \left(\frac{n_e}{10^{-3} \text{ cm}^{-3}} \right)^{-1} \text{ yr} \quad (3)$$

Equation (3) yields a life of 10^{10} yr for $n_e \sim 10^{-3}$, a reasonable intra-cluster value, at least in the outer regions with $\gamma = 10^3$.

The cosmic rays probably escape into the intra-cluster medium from the galaxies. Diffusion in a 10^{-11} T field is too slow, as is turbulent mixing of large-scale plasma at a speed similar to galaxy random motion. Instead, we appeal to galactic winds which move at $\sim 400 \text{ km s}^{-1}$ and which are likely to penetrate out to ~ 3 Mpc in 3×10^9 yr before being stopped by the pressure of the medium if the flow initially is 100 kpc in diameter. We suppose cosmic ray electrons to be transported by the winds. A possible origin of the electrons lies in supernova remnants, which may supply $10^{52}/1000$ erg in energetic particles. Since A1975 requires 3×10^{62} ergs in cosmic-ray electrons to supply the observed EUV flux, the supernova rate needs to be 100 per year in 100 large galaxies over 10^{10} years. Alternatively, consider an AGN origin of the cosmic rays using CYG A as the model, equating the 1.6×10^{44} erg/s radio emission with the energetic particle injection rate. Some 20 similar AGN producing cosmic-rays for $\sim 10^{10}$ yr at $z < 2$ would provide the required total energy in the cluster medium. The energetics of M87 make a convincing case for a cosmic-ray origin of the central EUV excess, despite the steep electron spectral index. Within 2 arc min of the centre, this excess emission is $L_{\text{EUV}} = 8 \times 10^{37}$ erg/s. The required cosmic-ray energy for inverse Compton emission in the EUV is

$$E_{\text{CR}} \approx 3 \times 10^{62} \frac{L_{\text{EUV}}}{10^{45}} \left(\frac{\gamma}{300} \right)^{-1} \text{ erg.} \quad (4)$$

yielding 2×10^{54} erg. Taking a suitably high value for the nearby intra-cluster density, $n_e \sim 10^{-2}$, gives a typical $\gamma \sim 300$ cosmic-ray electron life 10^9 yr. Further assuming an M87 cosmic-ray luminosity equal to the X-ray luminosity of $\approx 10^{43}$ erg/s, we expect M87 to pump 10^{59} ergs of relativistic electrons out into the intra-cluster medium in 10^9 yr. This value is well below the requirements for the IC mechanism, allowing a considerable inefficiency. 400 km/s Galactic winds would transport cosmic rays over 12kpc or the central 2' arc in 10^8 yr.

References

- Carpenter, G.F., *et al.* 1976, Proc. R. Soc. Lond. A35, 521
Harris, D.E. & Romanishin, W. 1974, ApJ 188, 209
Juda, M., *et al.* 1991, ApJ 367, 182
Krauss, L. 1997, in *The Identification Of Dark Matter*, Ed. N Spooner (World Scientific, Singapore)
Lieu, R., *et al.* 1992, ApJ 397, 158
Lieu, R., *et al.* 1996, Science 274, 1335
Sarazin, C.L., & R. Lieu, R. 1998, ApJ Lett. 494, 177
Schindler, S., & E. Muller, E. 1993 A&A 272, 137
Sidher, S.D., Sumner, T.J., Quenby, J.J., & Gambhir, M. 1996, A&A 305, 308
Sidher, S.D., Sumner, T.J., & Quenby, J.J. 1999, A & A 344, 333